

## Binding of Propylene Oxide to Porphyrin- and Salen-M(III) Cations, Where M = Al, Ga, Cr, and Co

Peter Chen,<sup>\*†</sup> Malcolm H. Chisholm,<sup>\*‡</sup> Judith C. Gallucci,<sup>‡</sup> Xiangyang Zhang,<sup>†</sup> and Zhiping Zhou<sup>‡</sup>

Department of Chemistry, The Ohio State University, 100 W. 18th Avenue, Columbus, Ohio 43210-1185, and Laboratorium für Organische Chemie, Eidgenössische Technische Hochschule (ETH), CH-8092 Zürich, Switzerland

Received October 7, 2004

The binding of propylene oxide (PO) to a series of metal cations LM(III)<sup>+</sup>, where for L = tetraphenylporphyrin (TPP) M = Al, Ga, Cr, and Co, and for L = (*R,R*)-*N,N'*-bis(3,5-di-*tert*-butylsalicylidene)-1,2-cyclohexanediamine (salen) M = Al and Cr, was studied in the gas phase by electrospray tandem mass spectroscopy, and the relative stabilities of LM(PO)<sub>2</sub><sup>+</sup> and LM(PO)<sup>+</sup> cations were determined. The chromium(III) and aluminum(III) cations most tenaciously bind PO, and for M = Al, coordination to the TPP ligated metal center was favored relative to salen. For (TPP)M(PO)<sub>2</sub><sup>+</sup>, the dissociation of PO followed the order M = Al > Cr, but for (TPP)M(PO)<sup>+</sup> the dissociation was M = Cr > Al. The single-crystal structural determinations on (*R,R*-salen)AlOCHMe(S)CH<sub>2</sub>Cl·0.5PO and (*R,R*-salen)AlO<sub>2</sub>CMe·1.5py grown in neat PO and pyridine, respectively, reveal five-coordinate aluminum(III) centers with the alkoxide/acetate ligands in the axial position of a square-based pyramid. These results are discussed in terms of the reactivity of these metal complexes in ring-opening polymerizations and copolymerizations with PO and CO<sub>2</sub>, respectively.

### Introduction

Catalytic reactions proceed via a series of elementary reactions, each of which is in principle reversible, and collectively these determine the turnover-limiting frequency that replaces what is commonly called a rate-limiting step for a reaction. In the ring-opening polymerization of epoxides by metal complexes and in the copolymerization of epoxides and carbon dioxide to give poly(alkene oxides) and poly(alkene carbonates), respectively, the coordination of the alkene oxide to the metal is one of the key steps.<sup>1–10</sup> Coordination to the Lewis acidic metal center facilitates ring opening by both an S<sub>N</sub>2 and an S<sub>N</sub>1 reaction pathway.<sup>11,12</sup>

\* To whom correspondence should be addressed. E-mail: chisholm@chemistry.ohio-state.edu (M.H.C.).

† Eidgenössische Technische Hochschule.

‡ The Ohio State University.

- (1) Darensbourg, D. J.; Holtcamp, M. W. *Coord. Chem. Rev.* **1996**, *153*, 155–174.
- (2) Super, M. S.; Beckman, E. J. *Trends Polym. Sci.* **1997**, *5*, 236–240.
- (3) Kuran, W. *Prog. Polym. Sci.* **1998**, *23*, 919–992.
- (4) Nozaki, K. *J. Polym. Sci. A: Polym. Chem.* **2003**, *42*, 215–221.
- (5) Rokicki, A.; Kuran, W. *J. Macromol. Sci., Rev. Macromol. Chem.* **1981**, *C21*, 135–186.
- (6) Nakano, K.; Kosaka, N.; Hiyama, T.; Nozaki, K. *Dalton Trans.* **2003**, 4039–4050.
- (7) Sigwalt, P. *Angew. Makromol. Chem.* **1981**, *94*, 161–180.
- (8) Tsuruta, T. *Pure Appl. Chem.* **1981**, *53*, 1745–1751.
- (9) Inoue, S. *J. Polym. Sci. A: Polym. Chem.* **2000**, *38*, 2861–2871.
- (10) Inoue, S. *Prog. Polym. Sci.* **1988**, *13*, 63–81.

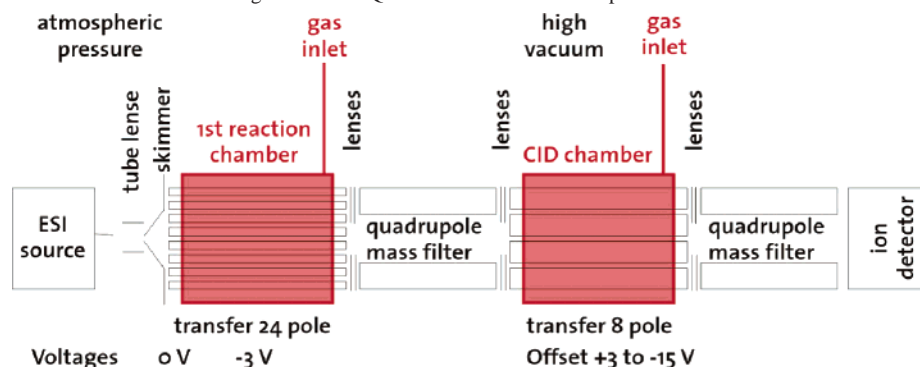
**Table 1.** Homopolymerization of PO by TPP–Metal Complexes<sup>a</sup>

entry	catal system	reacn time (h)	PPO <sup>b</sup> (%)	10 <sup>-3</sup> M <sub>n</sub> <sup>c</sup>	PDI <sup>c</sup>
1	(TPP)CrCl	120	76	61	1.53
2	(TPP)CrCl/DMAP <sup>d</sup>	120	59	44	1.38
3	(TPP)AlCl	168	50	28	1.32
4	(TPP)AlCl/DMAP	168	2		
5	(TPP)CoCl	120	<i>e</i>		
6	(TPP)CoCl/DMAP	120			

<sup>a</sup> The polymerization reactions were carried out in neat PO (2 mL) at 25 °C; [cat]:[PO] = 1:1500; 1 equiv of DMAP added if needed. No PPO was formed by using (TPP)GaCl and (salen)AlCl, and PPO could be formed by (salen)CrCl only at high [cat] and elevated temperatures. <sup>b</sup> Determined by <sup>1</sup>H NMR. <sup>c</sup> M<sub>n</sub> and PDI determined by gel permeation chromatography. <sup>d</sup> DMAP, 4-(dimethylamino)pyridine. <sup>e</sup> No or little formation.

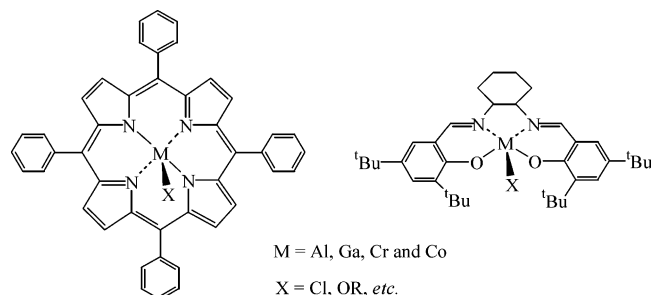
As is shown in Tables 1 and 2, various tetraphenylporphyrin- (TPP) and salen-metal(III) complexes (Figure 1) are effective in formation of poly(propylene oxide), PPO, and poly(propylene carbonate), PPC. There are, however, notable and quite remarkable differences between the activity of the metals Al(III), Cr(III), and Co(III), all of which have a very similar ionic radius, and between the porphyrin and salen ligands. We describe here studies of the binding of propylene oxide to the porphyrin and salen metal(III) cations,

- (11) Parker, R. E.; Isaacs, N. S. *Chem. Rev.* **1959**, *59*, 737–799.
- (12) March, J. *Advanced Organic Chemistry*, 4th ed.; 1992.

**Scheme 1.** Representation of the Modified Finnigan MAT TSQ-700 ESI Tandem Mass Spectrometer

**Table 2.** Copolymerization of PO/CO<sub>2</sub> by TPP- and salen-Metal Complexes<sup>a</sup>

entry	catal system	reacn time (h)	PPC <sup>b</sup> (%)	PPO <sup>c</sup> (%)	PC <sup>d</sup> (%)	10 <sup>-3</sup> M <sub>n</sub> <sup>e</sup>	PDI
1	(TPP)CrCl	48	8	92	<i>f</i>	85	1.49
2	(TPP)CrCl/DMAP	48	49	26		23	1.41
3	(TPP)AlCl	144	4	21		12	1.19
4	(TPP)AlCl/DMAP	144	57	7	1	31	1.24
5	(TPP)CoCl	48					
6	(TPP)CoCl/DMAP	48			3		
7	(salen)CrCl	144	13	1	1	9	1.21
8	(salen)CrCl/DMAP	144	25	1	2	14	1.35
9	(salen)AlCl	144					
10	(salen)AlCl/DMAP	144					
11 <sup>g</sup>	(salen)CoOAc	3	35			8	1.57

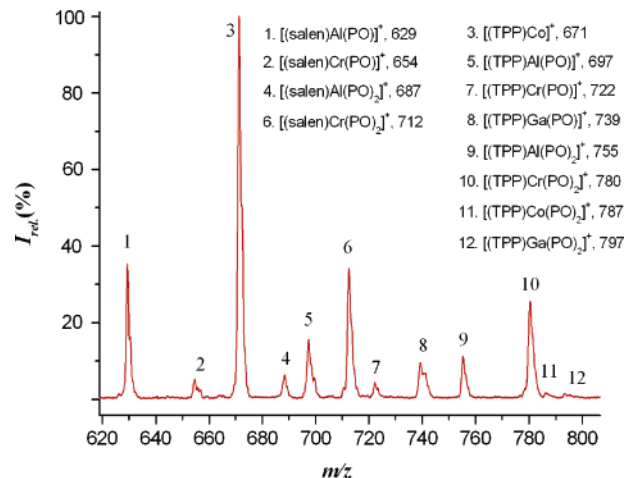
<sup>a</sup> The polymerization reactions were carried out in neat PO (2 mL) at 25 °C under 50 bar CO<sub>2</sub> pressure; [cat]:[PO] = 1:1500; 1 equiv of DMAP added if needed. <sup>b</sup> Carbonate linkages in the polymers obtained in the reaction mixtures determined by <sup>1</sup>H NMR. <sup>c</sup> Ether linkages in the resulting polymers determined by <sup>1</sup>H NMR. <sup>d</sup> Cyclic propylene carbonate in the products determined by <sup>1</sup>H NMR. <sup>e</sup> M<sub>n</sub> and PDI determined by gel permeation chromatography. <sup>f</sup> No or little formation. <sup>g</sup> Reference 30, [cat]:[PO] = 1:200.


**Figure 1.** Tetraphenylporphyrin- and salen-metal(III) complexes.

LM<sup>+</sup>, in the gas phase that clearly reveal the relative Lewis acidities of these ligated metal ions and furthermore their propensity to bind one or two neutral ligands. Finally, we report the molecular structures of *S*-PO, (*R,R*-salen)AlOCHMe-(*S*)CH<sub>2</sub>Cl, and (*R,R*-salen)AlO<sub>2</sub>CMe·1.5py that are relevant to the ring opening of PO by aluminum salen and porphyrin complexes.

## Results and Discussion

**Gas-Phase Studies. 1. Binding of Propylene Oxide.** We studied the binding of PO to the (TPP)M<sup>+</sup> cations by electrospray tandem mass spectrometry as depicted in Scheme 1.<sup>13</sup> In the first reaction chamber the (TPP)M<sup>+</sup> ions are allowed to react with PO (1 × 10<sup>-2</sup> Torr), and the


**Figure 2.** ESI/MS from the reactions between TPP-/salen-metal cations and propylene oxide in the gas phase.

resultant ions (TPP)M(PO)<sub>n</sub><sup>+</sup>, where *n* = 1 or 2, are detected and selected. As is shown in Figure 2, the cobalt cation has a very low affinity for PO and is present almost exclusively as (TPP)Co<sup>+</sup> with just a detectable amount of (TPP)Co(PO)<sub>2</sub><sup>+</sup>. This is a clear indication of the weaker Lewis acidity of (TPP)Co<sup>+</sup>. Aluminum forms both (TPP)Al(PO)<sub>n</sub><sup>+</sup> cations for *n* = 1 and 2 with a slight preference for *n* = 1, while for chromium the (TPP)Cr(PO)<sub>2</sub><sup>+</sup> cation is clearly much preferred. Also shown in Figure 2 are ions due to (TPP)Ga(PO)<sub>n</sub><sup>+</sup> (*n* = 1, 2) and related (salen)M(PO)<sub>n</sub><sup>+</sup>, where M = Al and Cr, and these will be discussed later. These PO adducts formed in the gas phase are not ring-opening derivatives as will be shown by their collision-induced displacement experiments; vide infra.

In the second reaction chamber the relative binding affinities of the (TPP)M(PO)<sub>n</sub><sup>+</sup> ions are examined by collision-induced dissociation (CID) experiments. A selected ion (TPP)M(PO)<sub>n</sub><sup>+</sup> (*n* = 1 or 2) at the same concentration is allowed to collide with xenon (3 × 10<sup>-5</sup> Torr) and the voltage is increased,<sup>14</sup> and the relative abundance of the ions (both the parent and daughter) are detected as shown in Scheme 1.

From the graphical data presented in Figure 3 we can conclude that for the ions containing one PO the ease of

(13) Chen, P. *Angew. Chem., Int. Ed.* **2003**, *42*, 2832–2847.

(14) The xenon pressure is relatively low to allow the single-collision experiments.

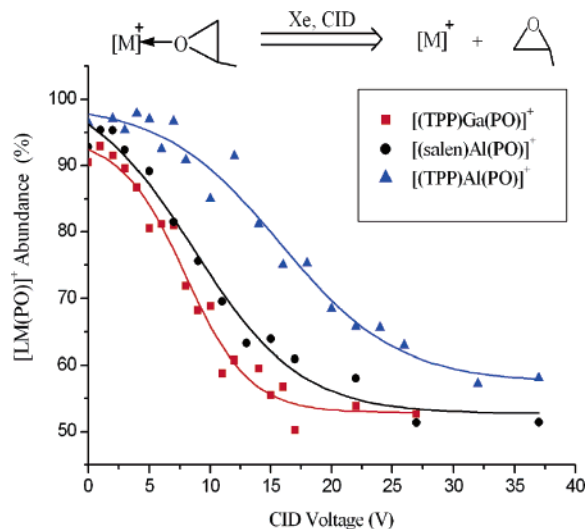


**Figure 3.** Plots of  $\text{LM(PO)}^+$  abundance versus CID voltage from the dissociation reaction of  $\text{LM(PO)}^+$  with xenon in the CID chamber ( $[\text{M}]^+ = \text{LM}^+$ ).

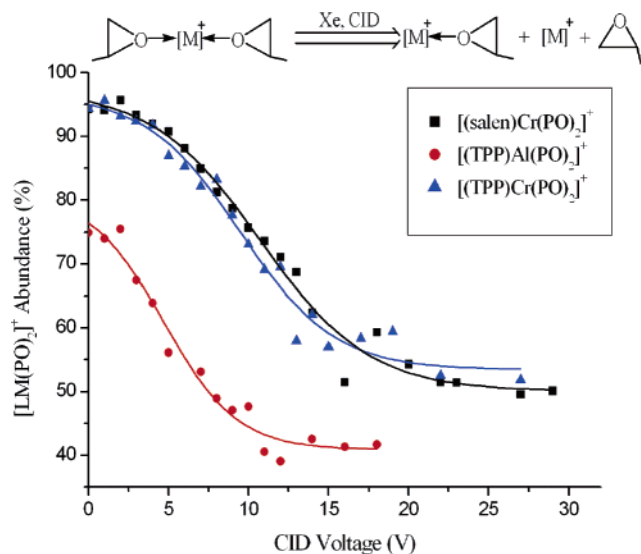


**Figure 4.** Plots of  $\text{LM(PO)}_2^+$  abundance versus CID voltage from the dissociation reactions of  $\text{LM(PO)}_2^+$  with xenon in the CID chamber ( $[\text{M}]^+ = \text{LM}^+$ ).

dissociation follows the order  $(\text{TPP})\text{Ga}^+ > (\text{salen})\text{Al}^+ > (\text{TPP})\text{Al}^+$ , which is the inverse order of their Lewis acidities. This makes good sense as gallium is notably softer than aluminum and element–element bond strengths decrease down a series in the main group. The difference in PO binding to the salen and porphyrin  $\text{Al}^+$  cations is also particularly noteworthy and reflects the fact that salen is a significantly stronger donor ligand relative to TPP. The  $(\text{TPP})\text{Al}^+$  cation is more Lewis acidic than its  $(\text{salen})\text{Al}^+$  counterpart. We could not examine  $(\text{TPP})\text{Cr(PO)}^+$  ion as its concentration was relatively too low. However, a comparison is seen for the bis PO adducts.

Figures 4 and 5 compare the  $(\text{TPP})\text{M(PO)}_2^+$  ( $\text{M} = \text{Al}, \text{Cr}$ ) and  $(\text{salen})\text{Cr(PO)}_2^+$  ions with respect to their dissociation of PO. Specifically in Figure 4 we can see the loss of the bis PO cations in the order  $(\text{TPP})\text{Al(PO)}_2^+ \gg (\text{TPP})\text{Cr(PO)}_2^+ \sim (\text{salen})\text{Cr(PO)}_2^+$ . This is a clear indication of the high affinity of the chromium(III) ion to retain six coordina-

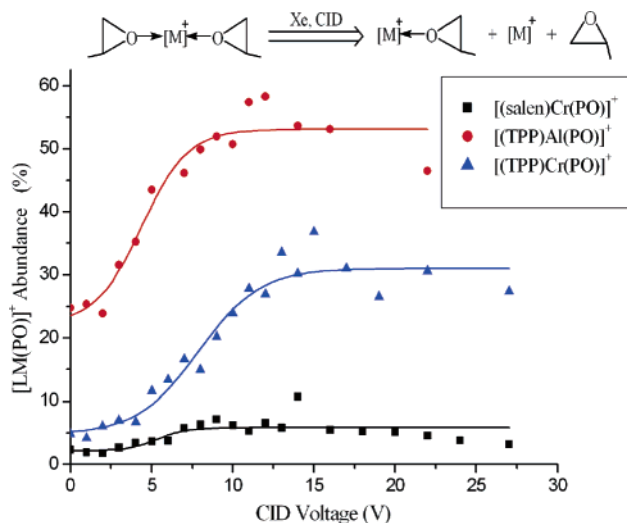


**Figure 5.** Plots of  $\text{LM(PO)}^+$  abundance versus CID voltage from the dissociation reactions of  $\text{LM(PO)}_2^+$  with xenon in the CID chamber ( $[\text{M}]^+ = \text{LM}^+$ ).

tion. In Figure 5, we show the appearance of the *mono* PO cations. Here we see the growth of  $(\text{TPP})\text{Al(PO)}^+ > (\text{TPP})\text{Cr(PO)}^+ > (\text{salen})\text{Cr(PO)}^+$  with the latter being at a maximum in the order of only 5%. From this we can conclude that the binding of PO to the four metal ions is in the order  $\text{Al} > \text{Cr}$  and that for chromium the TPP favors coordination relative to salen. For the chromium salen cations there is cooperative dissociation of PO. As shown in the following equation, for  $(\text{salen})\text{Cr(PO)}_2^+$ ,  $k_2 \gg k_1$  whereas, for  $(\text{TPP})\text{Al(PO)}_2^+$ , the initial loss of PO forms  $(\text{TPP})\text{Al(PO)}^+$  predominantly, i.e.,  $k_2 < k_1$ .



## 2. Ring Opening of Propylene Oxide in the Gas Phase.

Since the cationic mechanism for epoxide ring opening is well-known for some metal complexes,<sup>15–19</sup> we examined the possibility of a cationic pathway for PO ring-opening polymerization in the gas phase by the TPP and salen metal cations. As shown in Figure 2, no metal ions with PO adduct number  $> 2$  were detected. Furthermore, we examined the possibility of PO ring opening with the assist of neutral nucleophiles, such as diethylamine and pyridine. One cation, either  $\text{LM(PO)}^+$  or  $\text{LM(PO)}_2^+$ , was selected and reacted with the nucleophile ( $3 \times 10^{-4}$  Torr) in the CID chamber. Interestingly, ligand displacements were observed rather than PO ring opening as shown in Figure 6 in the case of pyridine. We should notice that the species in the gas phase are in an extremely low concentration relative to the solution phase, and these cations are not among the ones with strong Lewis

- Bochmann, M.; Lancaster, S. J.; Hannant, M. D.; Rodriguez, A.; Schormann, M.; Walker, D. A.; Woodman, T. J. *Pure Appl. Chem.* **2003**, *75*, 1183–1195.
- Entelis, S. G.; Korovina, G. *Makromol. Chem.* **1974**, *175*, 1253–1280.
- Munoz-Hernandez, M.-A.; McKee, M. L.; Keizer, T. S.; Yearwood, B. C.; Atwood, D. A. *J. Chem. Soc., Dalton Trans.* **2002**, 410–414.
- Jegier, J. A.; Munoz-Hernandez, M.-A.; Atwood, D. A. *J. Chem. Soc., Dalton Trans.* **1999**, 2583–2588.
- Inoue, M.; Sugita, T.; Kiso, Y.; Ichikawa, K. *Bull. Chem. Soc. Jpn.* **1976**, *49*, 1063–1071.

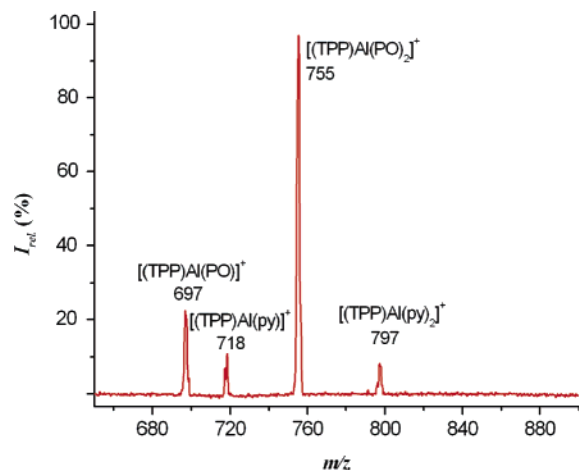


**Figure 6.** ESI/MS from the reaction of  $(\text{TPP})\text{Al}(\text{PO})_2^+$  with pyridine in the gas phase.

acidity. In fact, PO ring-opening polymerization was observed when a bimetallic cation of  $[(\text{salen})\text{Cr}]_2^{2+}$  was used in the experiment.<sup>20</sup>

**Polymerization Reactions in the Solution Phase.** As shown in Table 1 only the TPP-metal chlorides of aluminum and chromium are effective in polymerizing PO at room temperature and of these chromium is the more active. The addition of the strong nucleophile (strong Lewis base, 1 equiv) 4-(dimethylamino)pyridine, DMAP, suppresses the polymerization and for aluminum essentially renders the system inactive. The related cobalt complex with or without DMAP is essentially inactive. The salen metal chlorides of chromium and aluminum are also inactive at 25 °C with respect to homopolymerization of PO although both will ring open one molecule of PO.<sup>21,22</sup> However, at 75 °C in neat PO in a bomb the salen chromium becomes active.<sup>20</sup>

In Table 2 we present data pertaining to the copolymerization of PO and  $\text{CO}_2$ , where it is evident that the reactivity order is  $\text{M} = \text{Cr} > \text{Al} > \text{Co}$  and that the added DMAP favors the formation of PPC.<sup>23,24</sup> Indeed in its absence only a trace of  $\text{CO}_2$  is incorporated into the polymer which is largely PPO. Also we can see that the activity order on the attendant ligands is TPP > salen. We should note that Darensbourg and co-workers have extensively studied the salen-chromium system with respect to both changes of the ligand itself (backbone and aromatic ring) and Lewis base additives, and they recently reported that  $(\text{salen})\text{Ga}^{\text{III}}$  compounds were of little reactivity in the copolymerization of CHO and  $\text{CO}_2$ .<sup>25–29</sup> Also Coates has reported that salen

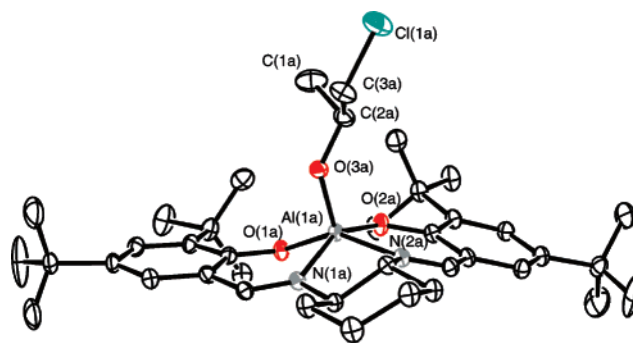


**Figure 7.** ORTEP view of  $(R,R\text{-salen})\text{AlOCHMe}(S)\text{CH}_2\text{Cl}$ .

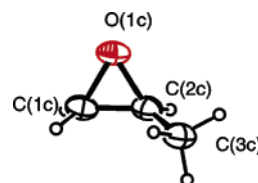


**Figure 8.** ORTEP view of *S*-propylene oxide. Selected bond distances (Å) and angles (deg): O(1c)–C(1c) 1.428(4), O(1c)–C(2c) 1.430(5), C(1c)–C(2c) 1.431(6), C(2c)–C(3c) 1.454(6); C(1c)–O(1c)–C(2c) 60.1(2), O(1c)–C(1c)–C(2c) 60.0(2), O(1c)–C(2c)–C(1c) 59.9(2), O(1c)–C(2c)–C(3c) 117.6(3), C(1c)–C(2c)–C(3c) 123.5(4).

**Table 3.** Selected Bond Distances (Å) and Angles (deg) for  $(R,R\text{-salen})\text{AlOCHMe}(S)\text{CH}_2\text{Cl}$

Al(1a)–O(1a)	1.800(2)	O(3a)–C(2a)	1.405(3)
Al(1a)–O(2a)	1.793(2)	C(1a)–C(2a)	1.540(5)
Al(1a)–O(3a)	1.736(2)	C(2a)–C(3a)	1.521(5)
Al(1a)–N(1a)	2.027(2)	Cl(1a)–C(3a)	1.806(3)
Al(1a)–N(2a)	2.007(2)		
O(3a)–Al(1a)–O(2a)	112.2(1)	O(1a)–Al(1a)–N(1a)	87.5(1)
O(3a)–Al(1a)–O(1a)	108.1(1)	N(2a)–Al(1a)–N(1a)	78.7(1)
O(2a)–Al(1a)–O(1a)	90.5(1)	C(2a)–O(3a)–Al(1a)	132.2(2)
O(3a)–Al(1a)–N(2a)	102.4(1)	O(3a)–C(2a)–C(3a)	105.3(2)
O(2a)–Al(1a)–N(2a)	87.8(1)	O(3a)–C(2a)–C(1a)	110.1(3)
O(1a)–Al(1a)–N(2a)	147.6(1)	C(3a)–C(2a)–C(1a)	111.3(3)
O(3a)–Al(1a)–N(1a)	96.0(1)	C(2a)–C(3a)–Cl(1a)	111.7(2)
O(2a)–Al(1a)–N(1a)	150.8(1)		

cobalt acetate is active in the formation of PPC,<sup>30</sup> and  $(\text{salen})\text{-Co}^{\text{III}}$  compounds have been extensively studied as catalysts in the hydrolytic kinetic resolution of terminal epoxides.<sup>31–33</sup>

**Solid-State and Molecular Structures.** The ring opening of *S*-PO by  $(R,R\text{-salen})\text{AlCl}$  yields two products:  $(R,R\text{-salen})\text{AlOCHMe}(S)\text{CH}_2\text{Cl}$  (**1**) as the major product;  $(R,R\text{-salen})\text{AlOCH}_2\text{CHMe}(R)\text{Cl}$  as the minor product (10%). The molecular structure of compound **1** was determined on a crystal grown in neat *S*-PO and is particularly pertinent to this study. In the solid state there are two five coordinate aluminum(III) centers that are nestled together in a head-tail salen packing motif as shown in Figure S1 in the Supporting Information. There is also one molecule of PO

(20) Shoen, E.; Zhang, X.; Zhou, Z.; Chisholm, M. H.; Chen, P., *Inorg. Chem.* **2004**, *43*, 7278–7280.

(21) Jacobsen, E. N. *Acc. Chem. Res.* **2000**, *33*, 421–431.

(22) Paddock, R. L.; Nguyen, S. T. *J. Am. Chem. Soc.* **2001**, *123*, 11498–11499.

(23) Aida, T.; Ishikawa, M.; Inoue, S. *Macromolecules* **1986**, *19*, 8–13.

(24) Jung, J. H.; Ree, M.; Chang, T. *J. Polym. Sci. A: Polym. Chem.* **1999**, *37*, 3329–3336.

(25) Darensbourg, D. J.; Mackiewicz, R. M.; Phelps, A. L.; Billodeaux, D. R. *Acc. Chem. Res.*, ACS ASAP.

(26) Darensbourg, D. J.; Mackiewicz, R. M.; Rodgers, J. L.; Phelps, A. L. *Inorg. Chem.* **2004**, *43*, 1831–1833.

(27) Darensbourg, D. J.; Yarbrough, J. C. *J. Am. Chem. Soc.* **2002**, *124*, 6335–6342.

(28) Darensbourg, D. J.; Yarbrough, J. C.; Ortiz, C.; Fang, C. C. *J. Am. Chem. Soc.* **2003**, *125*, 7586–7591.

(29) Darensbourg, D. J.; Billodeaux, D. R. *C. R. Chim.* **2004**, *7*, 755–761.

(30) Qin, Z.; Thomas, C. M.; Lee, S.; Coates, G. W. *Angew. Chem., Int. Ed.* **2003**, *42*, 5484–5487.

(31) Tohma, H. *Organomet. News* **1995**, 137.

(32) Tokunaga, M.; Larrow, J. F.; Kakiuchi, F.; Jacobsen, E. N. *Science* **1997**, *277*, 936–938.

(33) Nielsen, L. P. C.; Stevenson, C. P.; Blackmond, D. G.; Jacobsen, E. N. *J. Am. Chem. Soc.* **2004**, *126*, 1360–1362.

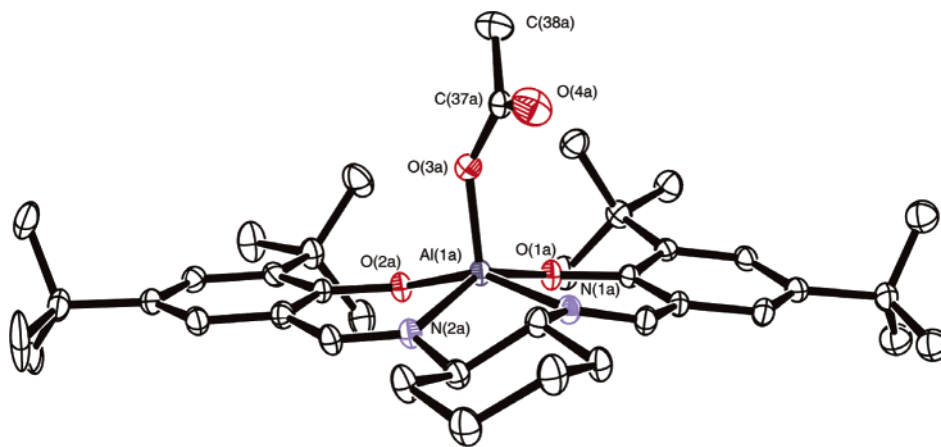


Figure 9. ORTEP view of (*R,R*-salen)AlOOCMe.

trapped in the lattice. The coordination about aluminum is best described as a square-based pyramid with the Al–OR (alkoxide) bond in the axial site. Figure 7 shows one of the two Al molecules in the unit cell. Selected bond distances are given in Table 3.

The molecule of *S*-PO is shown in Figure 8. This is the first X-ray structural determination of the free (unligated) PO molecule.<sup>34–36</sup> Pertinent bond distances and angles are given in the caption. What is particularly pertinent here is that the aluminum center remains five-coordinate even when PO is present as a solvent. For (salen)chromium azide Jacobsen reported the structure of the ring-opening product of cyclopentene oxide and found a solvent molecule of THF in the axial position.<sup>21,37</sup>

An alkoxide ligand is known to have a higher trans-influence than that of a carboxylate or alkyl carbonate ligand.<sup>38</sup> Consequently we investigated the ability of (salen)-AlO<sub>2</sub>CMe to bind a stronger Lewis base, namely pyridine. The molecular structure of this compound determined from a crystal grown in neat pyridine is shown in Figure 9. The aluminum is again five-coordinate, and the acetate ligand is in the apical position of a square-based pyramid. Significant note is the fact that the acetate is η<sup>1</sup>-coordinated. The long Al–O(acetate) distance is 3.45 Å, and the Al–O(acetate) bond of 1.77 Å is also longer than that in the related Al–O(alkoxide) bond (1.74 Å) (Tables 3 and 4). In the lattice there are two Al molecules and three noncoordinated pyridine molecules per unit cell (Figure S2). This is a clear indication that the Al(III) center is only weakly Lewis acidic. Of course, Al(III) six-coordinate ions are well-known and Atwood has shown that (salen)Al cations with weakly coordinating anions (OTs<sup>−</sup>, BPh<sub>4</sub><sup>−</sup>, etc.) will readily pick up two molecules of O-donor solvents, such as MeOH, THF, or H<sub>2</sub>O.<sup>17,18,39</sup>

Table 4. Selected Bond Distances (Å) and Angles (deg) for (*R,R*-salen)AlOOCMe

Al(1a)–O(1a)	1.776(2)	Al(1a)–N(2a)	2.002(3)
Al(1a)–O(2a)	1.795(2)	O(3a)–C(37a)	1.295(4)
Al(1a)–O(3a)	1.772(2)	O(4a)–C(37a)	1.210(4)
Al(1a)–N(1a)	1.998(3)	C(37a)–C(38a)	1.493(5)
O(3a)–Al(1a)–O(2a)	100.6(1)	O(2a)–Al(1a)–N(1a)	154.9(1)
O(3a)–Al(1a)–O(1a)	104.3(1)	O(1a)–Al(1a)–N(1a)	89.4(1)
O(2a)–Al(1a)–O(1a)	90.6(1)	N(2a)–Al(1a)–N(1a)	79.7(1)
O(3a)–Al(1a)–N(2a)	105.9(1)	C(37a)–O(3a)–Al(1a)	143.5(2)
O(2a)–Al(1a)–N(2a)	87.8(1)	O(3a)–C(37a)–C(38a)	114.3(3)
O(1a)–Al(1a)–N(2a)	149.5(1)	O(3a)–C(37a)–O(4a)	123.5(3)
O(3a)–Al(1a)–N(1a)	103.6(1)	O(4a)–C(37a)–C(38a)	122.1(3)

## Concluding Remarks

For a series of related ions LM<sup>+</sup>, the Lewis acidity order follows M = Cr(III) ~ Al(III) > Co(III). For the formation of the mono PO adducts LM(PO)<sup>+</sup>, the metal–PO bond strength follows the order Al > Cr. For the adducts LM-(PO)<sub>2</sub><sup>+</sup>, the loss of the first PO is in the order Al > Cr. These notable differences in the metal porphyrin complexes can be traced to the d<sup>n</sup> configuration effects of the M(III) ions, d<sup>0</sup> for Al, d<sup>3</sup> for Cr, and d<sup>6</sup> for Co.<sup>40</sup> The binding of PO to the (TPP)M<sup>+</sup> ions was also noted to be stronger relative to the respective (salen)M<sup>+</sup> ions, which is taken to indicate the better donor properties of salen relative to TPP. Finally, the structural characterizations of the (salen)AlOCHMeCH<sub>2</sub>Cl and (salen)AlO<sub>2</sub>CMe molecules in the presence of excess PO and pyridine, respectively, provide further testimony to the importance of five-coordination relative to six for the (salen)Al cation.

It is also of interest here to note the recent report of Darensbourg et al. on the binding of oxiranes to (Tp)CdO<sub>2</sub>-CMe, where Tp = hydrotris(3-phenylpyrazol-1-yl)borate.<sup>41</sup> These authors noted that the enthalpy of adduct formation varied little with variation of the oxiranes (PO, CHO, limonene oxide, norbornene oxide, pinene oxide, etc.). In no case, however, did the soft Cd(II) center cause ring opening of the oxirane.

(34) Darensbourg, D. J.; Holtcamp, M. W.; Khandelwal, B.; Klausmeyer, K. K.; Reibenspies, J. H. *J. Am. Chem. Soc.* **1995**, *117*, 538–539.

(35) Beckwith, J. D.; Tschinkl, M.; Picot, A.; Tsunoda, M.; Bachman, R.; Gabbaie, F. P. *Organometallics* **2001**, *20*, 3169–3174.

(36) Harder, S.; Boersma, J.; Brandsma, L.; Kanters, J. A.; Duisenberg, A. J. M.; Van Lenthe, J. H. *Organometallics* **1990**, *9*, 511–516.

(37) Hansen, K. B.; Leighton, J. L.; Jacobsen, E. N. *J. Am. Chem. Soc.* **1996**, *118*, 10924–10925.

(38) Coe, B. J.; Glenwright, S. J. *Coord. Chem. Rev.* **2000**, *203*, 5–80.

(39) Sahasrabudhe, S.; Yearwood, B. C.; Atwood, D. A.; Scott, M. J. *Inorg. Synth.* **2004**, *34*, 14–20.

(40) Kettle, S. F. A., Ed. *Physical Inorganic Chemistry: Coordination Chemistry Approach*; 1996; pp 31–38.

(41) Darensbourg, D. J.; Billodeaux, D. R.; Perez, L. M. *Organometallics* **2004**, *23*, 5286–5290.

With respect to this study and the homopolymerization of PO, the weaker Lewis acidity of the Co(III) ion would seem to be responsible for its lack of activity. The difference between chromium and aluminum where the activity order is  $\text{Cr} > \text{Al}$  may well reflect the greater affinity for six-coordination which would allow for a bimolecular pathway in [Cr], as has been shown by Jacobsen for (salen)- $\text{CrN}_3$  in asymmetric ring opening of epoxides.<sup>37</sup> However, different mechanisms may operate for different metal ions with different ligand sets and further speculation is not warranted. As noted in the Introduction, a catalytic cycle involves several elementary reaction steps and collectively these determine the turnover-limiting frequency. What we have established is the relative affinity of the Lewis acidic metal cationic centers toward propylene oxide.

## Experimental Section

All syntheses and solvent manipulations were carried out under a nitrogen atmosphere using standard Schlenk-line and drybox techniques. Solvents were dried in the standard procedures. Propylene oxide (Alfa Aesar) was distilled from calcium hydride. 5,10,15,20-Tetraphenylporphine (Acros), diethylaluminum chloride (1.0 M solution in hexane, Aldrich), trimethylaluminum (2.0 M solution in hexane, Aldrich), 4-(dimethylamino)pyridine (Aldrich), (*R,R*)-*N,N'*-bis(3,5-di-*tert*-butylsalicylidene)-1,2-cyclohexenediamine (Aldrich), ((*R,R*)-*N,N'*-bis(3,5-di-*tert*-butylsalicylidene)-1,2-cyclohexenediamino)aluminum chloride (Aldrich), and ((*R,R*)-*N,N'*-bis(3,5-di-*tert*-butylsalicylidene)-1,2-cyclohexenediamino)chromium chloride (Aldrich) were used as received. Chromium(II) chloride, cobalt(II) chloride, and gallium(III) chloride were purchased from Aldrich. Deuterated solvents were stored over 4 Å molecular sieves for 24 h prior to use.

**NMR Experiments.**  $^1\text{H}$  and  $^{13}\text{C}\{^1\text{H}\}$  NMR experiments were carried out with a Bruker DRX-500 (5 mm broad band probe) spectrometers, operating at proton Larmor frequencies of 500 MHz. The parameters used in  $^{13}\text{C}\{^1\text{H}\}$  NMR experiments on the Bruker DRX-500 spectrometer were number of data points, TD = 65 536, sweep width, SWH = 1502 Hz, relaxation time, D1 = 2 s, and chemical shift range, 0–200 ppm. Their peak frequencies were referenced against the solvent, chloroform-*d* at 7.24 ppm for  $^1\text{H}$  and 77.0 ppm for  $^{13}\text{C}\{^1\text{H}\}$  NMR.

**Gel Permeation Chromatography.** Gel permeation chromatographic (GPC) analysis was performed at 35 °C on a Waters Breeze system equipped with a Waters 410 refractive index detector and a set of two columns, Waters Styragel HR-2 and HR-4 (Milford, MA). THF (HPLC grade) was used as the mobile phase at 1.0 mL/min. The sample concentration was 0.1%, and the injection volume was 100  $\mu\text{L}$ . The samples were centrifuged and filtered before analysis. The calibration curve was made with six polystyrene standards covering the molecular weight range from 580 to 460 000 Da.

**Mass Spectrometry/Gas-Phase Studies.** The complexes are typically diluted to  $10^{-5}$  M with  $\text{CH}_2\text{Cl}_2$  and electrosprayed on a modified Finnigan MAT TSQ-700 tandem mass spectrometer (Scheme 1) at a flow rate of 7–15 mL  $\text{min}^{-1}$  and at a potential of 4–5 kV using nitrogen as sheath gas. The ions are then passed through a heated capillary (typically at 150 °C) where they are declustered and the remaining solvent molecules are removed by high vacuum. The extent of desolvation and collisional activation can further be controlled by a tube lens potential, which typically ranges from 50 V (soft condition) to 120 V (hard condition). In

this work even harder desolvation conditions were used to get strong signal, e.g., tube lens  $\sim 150$  V. The transfer 24-pole (O1) acts as an ion guide to separate the ions from neutral molecules which are pumped off by a turbo pump located underneath the octopole. O1 is fitted with an open cylindrical sheath around the rods into which, depending on the setup used, a collision gas can be bled for thermalization or reaction at pressures up to 100 mTorr. Modification of normal octopole by a 37 cm radio frequency (rf) 24-pole is based on requirements of the longer reaction time and bigger pressure of reagent gas. The ions then enter the actual mass spectrometer, which is at  $10^{-6}$  Torr and 70 °C manifold temperature during operation. The configuration is quadrupole/octopole/quadrupole (Q1/O2/Q2), with the two quadrupoles as mass selection stages and the second octopole operating as a collision-induced dissociation (CID) cell. Spectra can be recorded in different modes. In the normal ESMS mode, only one quadrupole is operated (either Q1 or Q2), and a mass spectrum of the electrosprayed ions is recorded. This mode serves primarily to characterize the ions produced by a given set of conditions. In the daughter-ion mode, Q1 is used to mass-select ions of a single mass-to-charge-ratio from among all of the ions produced in O1, which are then collided or reacted with a target gas in O2 (CID cell) and finally mass-analyzed by Q2. This mode is used to obtain structural information (by analysis of the fragments) or the specific reactivity of a species of a given mass. Therefore, collision-induced dissociation (CID) could be done in either the radio frequency (rf) 24-pole ion guide by collision with Xe (0.08 Torr) or in a gas-filled (0.1 mTorr of either Xe or reagent gas) rf octopole ion guide. CID and ion–molecule reactions were all performed at low collision energy, i.e., –10 to –50 V in the laboratory frame.

**X-ray Crystallographic Studies.** The data collection crystals for (salen)AlOCHMeCH<sub>2</sub>Cl and (salen)AlOOCMe were both yellow chunks, which had been cut from a large crystal. Examination of the diffraction pattern on a Nonius Kappa CCD diffractometer indicated a triclinic crystal system. All work was done at 200 K using an Oxford Cryosystems cryostream cooler. The data collection strategy was set up to measure a hemisphere of reciprocal space with a redundancy factor of 3.1 for (salen)AlOCH<sub>2</sub>CHMeCl and 3.4 for (salen)AlOOCMe, which means that 90% of the reflections were measured at least 3.1 and 3.4 times, respectively. A combination of  $\phi$  and  $\omega$  scans with a frame width of  $1.0^\circ$  was used. Data integration was done with Denzo, and scaling and merging of the data was done with Scalepack.<sup>42</sup> Merging the data (but not the Friedel pairs) resulted in an  $R_{\text{int}}$  value of 0.036.

The structure of (salen)AlOCHMeCH<sub>2</sub>Cl was solved in *P1* by the direct methods in SHELXS-97.<sup>43</sup> The asymmetric unit contains two molecules of the Al complex and one solvent molecule of propylene oxide. The Al complexes are labeled as molecules A and B. One of the *tert*-butyl groups on molecule B was rotationally disordered and was modeled as two isotropic sets of atoms.

The structure of (salen)AlOOCMe was solved in *P1* by the direct methods in SHELXS-97. The asymmetric unit contains two molecules of the Al complex and three molecules of pyridine. The Al complexes are labeled as molecules A and B. Some of the *tert*-butyl groups were rotationally disordered and were modeled as two isotropic sets of atoms. For two of the three pyridine molecules (labeled as C and E), the location of the nitrogen atom was found by initially naming all of the atoms as carbon and then seeing which atom had the smallest refined isotropic *U* value. This atom was then changed to a nitrogen atom. For the third pyridine ring (labeled

(42) Otwinowski, Z.; Minor, W. *Methods Enzymol.* **1997**, 276, 307–326.

(43) Sheldrick, G. M.; Schneider, T. R. *Methods Enzymol.* **1997**, 277, 319–343.

**Table 5.** Crystallographic Details for (salen)AlOCHMeCH<sub>2</sub>Cl·0.5PO and (salen)AlOOCMe·1.5py

	(salen)AlOCHMeCH <sub>2</sub> Cl·0.5PO	(salen)AlOOCMe·1.5py
empirical formula	C <sub>39</sub> H <sub>58</sub> AlClN <sub>2</sub> O <sub>3</sub> + 1/2C <sub>3</sub> H <sub>6</sub> O	C <sub>38</sub> H <sub>55</sub> AlN <sub>2</sub> O <sub>3</sub> + 3/2C <sub>5</sub> H <sub>5</sub> N
fw	694.34	749.47
temp (K)	200	200
wavelength (Å)	0.710 73	0.710 73
cryst system	triclinic	triclinic
space group	P1	P1
unit cell dimens		
<i>a</i> (Å)	12.776(1)	12.554(1)
<i>b</i> (Å)	13.096(1)	12.887(1)
<i>c</i> (Å)	13.855(1)	14.614(1)
β (deg)	63.234(3)	85.652(3)
<i>V</i> (Å <sup>3</sup> )	1990.7(3)	2151.1(3)
<i>Z</i>	2	2
<i>D</i> <sub>calc</sub> (mg m <sup>-3</sup> )	1.158	1.157
abs coeff (mm <sup>-1</sup> )	0.157	0.092
<i>F</i> (000)	752	810
cryst size (mm <sup>-3</sup> )	0.27 × 0.31 × 0.42	0.27 × 0.35 × 0.35
θ range for data collcn (deg)	1.71–27.46	2.07–25.04
index ranges	−16 ≤ <i>h</i> ≤ 16, −16 ≤ <i>k</i> ≤ 16, −17 ≤ <i>l</i> ≤ 17	−14 ≤ <i>h</i> ≤ 14, −15 ≤ <i>k</i> ≤ 15, −17 ≤ <i>l</i> ≤ 17
reflens collcd	54 924	49 416
indpdt reflns	17 967 [R <sub>int</sub> = 0.036]	14 712 [R <sub>int</sub> = 0.035]
refinement method	full-matrix least squares on <i>F</i> <sup>2</sup>	full-matrix least squares on <i>F</i> <sup>2</sup>
data/restraints/params	17 967/3/894	14 712/66/985
Flack param	0.01(6)	0.03(15)
goodness-of-fit on <i>F</i> <sup>2</sup>	1.029	1.041
final <i>R</i> indices [ <i>I</i> > 2σ( <i>I</i> )]	R1 = 0.0572, wR2 = 0.1451	R1 = 0.0526, wR2 = 0.1324
<i>R</i> indices (all data)	R1 = 0.0768, wR2 = 0.1569	R1 = 0.0671, wR2 = 0.1420
largest diff peak and hole (e/Å <sup>3</sup> )	0.588 and −0.592	0.493 and −0.312

as D), the location of the nitrogen atom was not obvious with this method, and so all of the atoms were designated as carbon atoms.

Experimental data relating to both structure determinations are displayed in Table 5. CCDC 243038 and CCDC 245186 contain the supplementary crystallographic data for (*R,R*-salen)AlOCHMeCH<sub>2</sub>Cl and (*R,R*-salen)AlOOCMe, respectively. These data can be obtained free of charge via [www.ccdc.cam.ac.uk/data\\_request/cif](http://www.ccdc.cam.ac.uk/data_request/cif), by e-mailing [data\\_request@ccdc.cam.ac.uk](mailto:data_request@ccdc.cam.ac.uk).

**Synthesis of TPP–Aluminum Chloride.** (TPP)AlCl was prepared according to the literature.<sup>44,45</sup> To a solution of (TPP)H<sub>2</sub> (1.0 g, 1.6 mmol) in 30 mL of dichloromethane was added a solution of diethylaluminum chloride (Et<sub>2</sub>AlCl 1.0 M solution in hexane, 1.8 mL, 1.8 mmol). The addition was done slowly at room temperature. The resulting solution was left stirring 3 h after which the volatile fractions were removed under vacuum to give a purple powder in 85% yield. <sup>1</sup>H NMR (CDCl<sub>3</sub>, δ, ppm): 7.7, 8.2, 9.0 (aromatic). <sup>13</sup>C{<sup>1</sup>H} NMR (CDCl<sub>3</sub>, δ, ppm): 120.73, 126.95, 128.06, 132.39, 134.23, 141.14, 148.51 (aromatic). ESI/MS data: *m/z* = 639, (TPP)Al<sup>+</sup>.

**Synthesis of TPP–Chromium Chloride.** (TPP)CrCl was prepared according to the literature.<sup>46,47</sup> (TPP)H<sub>2</sub> (2.38 g, 3.9 mmol) was added to 200 mL of dimethylformamide (DMF). The mixture was stirred under reflux at 170 °C. After 10 min the (TPP)H<sub>2</sub> was dissolved and an excess of CrCl<sub>2</sub> (0.75 g, 6.1 mmol) was added to the refluxing solution. After 20 min, an aliquot was taken from the mixture for UV–vis. The spectrum showed free (TPP)H<sub>2</sub> still remained in solution. A further addition of CrCl<sub>2</sub> (0.5 g) was added to the solution, refluxing for another 20 min. No free (TPP)H<sub>2</sub> was found in UV–vis measurement. The reaction mixture was allowed to cool to room temperature and poured into 400 mL of ice-cold water. After the solid was filtered out and washed three times with

water, it was dried under vacuum at 100 °C. The crude product was purified by column chromatography with CHCl<sub>3</sub> as the eluent over alumina column. After CHCl<sub>3</sub> was removed, the product was dried overnight under vacuum at 100 °C, yielding 1.95 g of product. UV–vis spectroscopy was used to confirm the formation of (TPP)–CrCl.<sup>46</sup> ESI/MS data: *m/z* = 664, (TPP)Cr<sup>+</sup>.

**Synthesis of TPP–Cobalt Chloride.** (TPP)CoCl was prepared according to the literature.<sup>47,48</sup> (TPP)H<sub>2</sub> (1.5 g, 2.4 mmol) was added to 200 mL of DMF. The mixture was stirred under reflux at 170 °C. After 10 min the (TPP)H<sub>2</sub> was dissolved and an excess of CoCl<sub>2</sub> (0.4 g, 3.1 mmol) was added to the refluxing solution. After 30 min, an aliquot was taken from the mixture for UV–vis. The spectrum showed free (TPP)H<sub>2</sub> still remained in solution. A further addition of CoCl<sub>2</sub> (0.4 g) was added to the solution, refluxing for another 30 min. No free (TPP)H<sub>2</sub> was found in the UV–vis measurement. The reaction mixture was allowed to cool to room temperature and poured into 300 mL of concentrated HCl/MeOH solution overnight. After the removal of solvents and washing with a large amount of water, a purple solid was obtained and dried under vacuum at 100 °C. The crude product was purified by column chromatography with CH<sub>2</sub>Cl<sub>2</sub> (5% MeOH) as the eluent over silica column. After solvents were removed, the product was dried overnight under vacuum at 100 °C, yielding 1.25 g of product. UV–vis spectroscopy was used to confirm the formation of (TPP)CoCl.<sup>49</sup> <sup>1</sup>H NMR (CDCl<sub>3</sub>, δ, ppm): 7.70, 8.19, 8.70 (aromatic). ESI/MS data: *m/z* = 671, (TPP)Co<sup>+</sup>.

**Synthesis of TPP–Gallium Chloride.** (TPP)GaCl was prepared according to the literature.<sup>50,51</sup> (TPP)H<sub>2</sub> (0.25 g, 0.4 mmol), anhydrous sodium acetate (0.8 g, 9.6 mmol), and GaCl<sub>3</sub> (0.2 g, 1.1

(44) Aida, T.; Inoue, S. *J. Am. Chem. Soc.* **1983**, *105*, 1304–1309.

(45) Aida, T.; Wada, K.; Inoue, S. *Macromolecules* **1987**, *20*, 237–241.

(46) Summerville, D. A.; Jones, R. D.; Hoffman, B. M.; Basolo, F. *J. Am. Chem. Soc.* **1977**, *99*, 8195–8202.

(47) Adler, A. D.; Longo, F. R.; Kampas, F.; Kim, J. *J. Inorg. Nucl. Chem.* **1970**, *32*, 2443–2445.

(48) Sakurai, T.; Yamamoto, K.; Naito, H.; Nakamoto, N. *Bull. Chem. Soc. Jpn.* **1976**, *49*, 3042–3046.

(49) Sugimoto, H.; Ueda, N.; Mori, M. *Bull. Chem. Soc. Jpn.* **1981**, *54*, 3425–3432.

(50) Witowska-Jarosz, J.; Gorski, L.; Malinowska, E.; Jarosz, M. *J. Mass Spectrom.* **2002**, *37*, 1236–1241.

(51) Kadish, K. M.; Cornillon, J. L.; Coutsolelos, A.; Guillard, R. *Inorg. Chem.* **1987**, *26*, 4167–4173.

mmol) were added to 100 mL of acetic acid. The mixture was stirred and refluxed overnight at 120 °C. The reaction mixture was allowed to cool to room temperature. After the removal of acetic acid, the product was extracted with CHCl<sub>3</sub>. The crude product was purified by column chromatography with CHCl<sub>3</sub> as the eluent over an alumina column. After CHCl<sub>3</sub> was removed, the product was dried overnight under vacuum at 100 °C, yielding 0.15 g of product. UV-vis spectroscopy was used to confirm the formation of (TPP)GaCl.<sup>51</sup> <sup>1</sup>H NMR (CDCl<sub>3</sub>, δ, ppm): 7.76, 8.20, 9.07 (aromatic). ESI/MS data: *m/z* = 681, (TPP)Ga<sup>+</sup>.

**Synthesis of *R,R*-salen-Aluminum Acetate.** To a solution of (*R,R*-salen)H<sub>2</sub> (2.0 g, 3.7 mmol) in 20 mL of dichloromethane was added a solution of trimethylaluminum (AlMe<sub>3</sub> 2.0 M solution in hexane, 2.0 mL, 4.0 mmol), and the mixture was stirred for 3 h at room temperature. A yellow powder was obtained after the removal of volatile fractions under vacuum. The powder was redissolved in hexane, followed by the addition of 0.25 mL of acetic acid (4.4 mmol), and stirred for overnight. A yellow precipitate was obtained as the product (1.7 g). Crystals of this complex for X-ray measurement were obtained by slow evaporation of the solvent from a concentrated pyridine solution of the complex. <sup>1</sup>H NMR (CDCl<sub>3</sub>, δ, ppm): 1.79 (s, CH<sub>3</sub>COO), 1.29 (d, C(CH<sub>3</sub>)), 1.50 (s, C(CH<sub>3</sub>)), 1.44, 2.05, 2.41, 2.56, 3.09, 4.01 (cyclohexyl), 7.02, 7.09, 7.51 (aromatic), 8.18, 8.36(HC=N). Anal. Calcd: C, 72.35; H, 8.79; N, 4.44. Found: C, 72.21; H, 8.66; N, 4.35.

**Reactions between (*R,R*-salen)AlCl and *S*-PO.** A 0.5 g (0.8 mmol) amount of (*R,R*-salen)AlCl was allowed to react with 4 mL (57 mmol) of neat *S*-PO in 10 mL of CH<sub>2</sub>Cl<sub>2</sub> for 2 h at room temperature. A yellow powder was obtained after the removal of the excess of PO and solvent under vacuum. The products were analyzed by <sup>1</sup>H NMR. The major regioisomer was obtained by recrystallization of the product in toluene. Crystals of (*R,R*-salen)-

AlOCH(S)MeCH<sub>2</sub>Cl for X-ray measurement were obtained by slow evaporation of the solvent from a concentrated *S*-PO solution of the complex.

**Homopolymerization Reactions of PO.** In a typical reaction, 0.02 mmol of catalyst was allowed to react in 2 mL of neat PO (28.6 mmol) in a flask at room temperature, with addition of 2.4 mg of DMAP (0.02 mmol) if needed. After a certain time, the resulting mixture was analyzed by <sup>1</sup>H NMR. Then the reaction was quenched by adding methanol/HCl solution, and the obtained polymer was analyzed by gel permeation chromatography.

**Copolymerization Reactions of PO/CO<sub>2</sub>.** In a typical reaction, 0.02 mmol of catalyst was allowed to react in 2 mL of neat PO (28.6 mmol) in a stainless steel reaction vessel (Parr) under 50 bar CO<sub>2</sub> pressure at room temperature, with addition of 2.4 mg of DMAP (0.02 mmol) if needed. After a certain time, the resulting mixture was analyzed by <sup>1</sup>H NMR. Then the reaction was quenched by adding methanol/ HCl solution, and the obtained polymer was analyzed by gel permeation chromatography.

**Acknowledgment.** We thank the U.S. Department of Energy, Office of Basic Sciences, Chemistry Division, for financial support of this work at OSU and the Swiss National Science Foundation as well as the Research Commission at the ETH Zürich for support in Zürich. Z.Z. thanks The Ohio State University for an international travel grant.

**Supporting Information Available:** Crystallographic data and ORTEP views for (*R,R*-salen)AlOCHMe(*S*)CH<sub>2</sub>Cl·(0.5PO) and (*R,R*-salen)Al(O<sub>2</sub>CMe)·(1.5py). This material is available free of charge via the Internet at <http://pubs.acs.org>.

IC048597X